Article

Brain Iron Deficiency Changes the Stoichiometry of Adenosine Receptor Subtypes in Cortico-Striatal Terminals: Implications for Restless Legs Syndrome

Matilde S. Rodrigues [1], Samira G. Ferreira [1], César Quiroz [2], Christopher J. Earley [3], Diego García-Borreguero [4], Rodrigo A. Cunha [1,5], Francisco Ciruela [6,7], Attila Köfalvi [1] and Sergi Ferré [2,*]

1   CNC-Center for Neuroscience and Cell Biology of Coimbra, University of Coimbra, 3004-504 Coimbra, Portugal; matildesgcr@gmail.com (M.S.R.); carsamira@gmail.com (S.G.F.); rcunha@fmed.uc.pt (R.A.C.); akofalvi@gmail.com (A.K.)
2   Integrative Neurobiology Section, National Institute on Drug Abuse, Baltimore, MD 21224, USA; cesar.quiroz-molina@nih.gov
3   Department of Neurology, Johns Hopkins University, Baltimore, MD 21224, USA; cearley@jhmi.edu
4   Sleep Research Institute, 28036 Madrid, Spain; dgb@iis.es
5   Faculty of Medicine, University of Coimbra, 3004-504 Coimbra, Portugal
6   Pharmacology Unit, Department of Pathology and Experimental Therapeutics, Faculty of Medicine and Health Sciences, Institute of Neurosciences, University of Barcelona, 08907 L'Hospitalet de Llobregat, Spain; fciruela@ub.edu
7   Neuropharmacology and Pain Group, Neuroscience Program, Institut d'Investigació Biomèdica de Belvitge, Idibell, 08907 L'Hospitalet de Llobregat, Spain
*   Correspondence: sferre@intra.nida.nih.gov

Publisher's Note: MDPI stays neutral with regard to jurisdictional claims in published maps and institutional affiliations.

Abstract: Brain iron deficiency (BID) constitutes a primary pathophysiological mechanism in restless legs syndrome (RLS). BID in rodents has been widely used as an animal model of RLS, since it recapitulates key neurochemical changes reported in RLS patients and shows an RLS-like behavioral phenotype. Previous studies with the BID-rodent model of RLS demonstrated increased sensitivity of cortical pyramidal cells to release glutamate from their striatal nerve terminals driving striatal circuits, a correlative finding of the cortical motor hyperexcitability of RLS patients. It was also found that BID in rodents leads to changes in the adenosinergic system, a downregulation of the inhibitory adenosine A_1 receptors (A_1Rs) and upregulation of the excitatory adenosine A_{2A} receptors (A_{2A}Rs). It was then hypothesized, but not proven, that the BID-induced increased sensitivity of cortico-striatal glutamatergic terminals could be induced by a change in A_1R/A_{2A}R stoichiometry in favor of A_{2A}Rs. Here, we used a newly developed FACS-based synaptometric analysis to compare the relative abundance on A_1Rs and A_{2A}Rs in cortico-striatal and thalamo-striatal glutamatergic terminals (labeled with vesicular glutamate transporters VGLUT1 and VGLUT2, respectively) of control and BID rats. It could be demonstrated that BID (determined by measuring transferrin receptor density in the brain) is associated with a selective decrease in the A_1R/A_{2A}R ratio in VGLUT1 positive-striatal terminals.

Keywords: adenosine A_1 receptor; adenosine A_{2A} receptor; restless legs syndrome; brain iron deficiency; striatum; cortico-striatal terminals; thalamo-striatal terminals

1. Introduction

Restless legs syndrome (RLS) is a common sensorimotor disorder, whose basic components include a primary sensory experience, akathisia (an urgent need to move), and in about 80% of patients a secondary motor component, periodic leg movements during sleep (PLMS), can be found [1,2]. It has been postulated that the overlying framework of the disease is a biological bias toward maintaining alertness even in the face of severe

sleepiness [3]. It is generally accepted that brain iron deficiency (BID) is one of the primary pathophysiological mechanisms in RLS [2–4]. In fact, BID in rodents recapitulates key neurochemical changes reported in RLS patients and shows an RLS-like behavioral phenotype [3,4]. These neurochemical changes include presynaptic hyperdopaminergic and hyperglutamatergic states [2–4]. Utilization of the BID-rodent model of RLS could allow the identification of new neurochemical pathways and changes not previously reported in the human condition. Alterations in the adenosinergic system found in the BID rodent model [3,5] was an important new translational finding that led to a new potential treatment for RLS [6,7].

More specifically, BID in rodents was found to differentially modify the levels of the main adenosine receptor subtypes in the brain, downregulating and upregulating the levels of A_1 receptors (A_1Rs) and A_{2A} receptors (A_{2A}Rs), respectively [8,9]. The changes in A_1R density were found both in the cortex and striatum and occurred under a less severe iron-deficient (ID) diet, as compared with the changes in A_{2A}R density, which only occurred with a more severe ID diet [9]. The generalized decrease in A_1R density was then interpreted as a hypoadenosinergic state, and it was hypothesized to account for both the reported hyperdopaminergic and hyperglutamatergic states in RLS [3,5]. In fact, it is well established that A_1Rs mediate the universal adenosine-mediated inhibitory control of glutamatergic transmission in the brain [10]; A_1Rs are also indirectly and directly involved in the adenosine-mediated brake of dopaminergic transmission [11,12]. A generalized A_1R-dependent hypoadenosinergic state could provide the basis for the sensory-motor symptoms of RLS (akathisia and PLMS) and, since A_1Rs are involved in the homeostatic sleep mechanism [13], could also account for the biological bias toward alertness/arousal seen in RLS.

A specific correlative finding of the hyperglutamatergic state of RLS was the demonstration in the BID-rodent model of an increased sensitivity of cortical pyramidal cells to release glutamate by their efferent striatal nerve terminals [14]. The functional isolation of these terminals, using an in vivo optogenetic-microdialysis technique, demonstrated that they are targets of drugs with therapeutic efficacy in RLS, including the dopaminergic compounds pramipexole and ropinirole and the $\alpha_2\delta$ ligand gabapentin [2,15]. The three compounds significantly counteracted glutamate release by cortico-striatal terminals from rats with BID [14], and their efficacy most probably depends on the presence of presynaptic inhibitory dopamine receptors (D_2 and D_4 subtypes) and voltage-dependent calcium channels expressing $\alpha2\delta$ units [14,16].

Importantly for the adenosine perspective, striatal glutamatergic terminals are also endowed with A_1Rs and A_{2A}Rs, which we previously demonstrated to form A_1R-A_{2A}R complexes (heteromers) [17]. It was proposed that these A_1R-A_{2A}R heteromers provide a mechanism to fine-tune modulation of striatal glutamate release, whereby low concentrations of adenosine would preferentially activate A_1Rs, promoting inhibition of glutamate release, while high concentrations would activate A_{2A}Rs. As occurs in different brain glutamatergic synapses, the activation of A_{2A}Rs would promote glutamate release by allosterically counteracting A_1R activation in the A_1R-A_{2A}R heteromer and directly through adenylyl cyclase signaling [17–19]. A recently reported functionally important property of the A_1R-A_{2A}R heteromer is the loss of constitutive activity of the A_{2A}R [20]. We therefore hypothesized that changes in the density of A_1R and A_{2A}R in cortico-striatal glutamatergic terminals could be involved in the BID-induced increased activity of cortico-striatal terminals. Downregulation of A_1Rs should lead to a decrease in the ability of low basal concentrations of adenosine to tonically inhibit glutamate release, but also to an increase in the population of A_{2A}Rs not forming heteromers and, therefore, showing constitutive activity, a mechanism that would be more relevant upon concomitant upregulation of A_{2A}Rs.

That changes in A_1R/A_{2A}R stoichiometry in favor of A_{2A}Rs could be involved in the BID-induced increased sensitivity activity of striatal terminals was supported by a recent study that also used the in vivo optogenetic-microdialysis technique. It was first shown that an A_1R antagonist, which counteracts the activation of A_1Rs by endogenous

basal levels of adenosine, increases the sensitivity of cortico-striatal terminals to release glutamate [21]. In addition, increasing the extracellular levels of adenosine by application of dipyridamole, an inhibitor of equilibrative nucleoside transporters ENT1 and ENT2, inhibited basal and optogenetically-induced glutamate release by cortico-striatal terminals from rats with BID and controls [21]. These preclinical results predicted a possible clinical role of dipyridamole in RLS, which we could confirm in two recent clinical studies [6,7]. However, the actual BID-induced change in the $A_1R/A_{2A}R$ stoichiometry in cortico-striatal terminals still needs to be demonstrated. In the present study we directly address this question by using a newly developed FACS-based synaptometric analysis to compare the relative abundance on A_1Rs and $A_{2A}Rs$ in cortico-striatal glutamatergic terminals of control and BID rats.

2. Results

2.1. Diet-Induced Anemic Phenotype and Bid

As shown in Table 1, rats fed with the iron deficient diet (n = 11) showed a classical anemic phenotype, including a 16% reduction in body weight, severe reduction in red blood cell- and hemoglobin-related parameters, hypolymphocytemia, thrombocytopenia and a 91% reduction in serum iron content, as compared with controls (n = 10). The concomitant decrease in the level of iron in the brain can be determined by directly measuring the iron content or indirectly, as here documented, by analyzing the density or expression of the transferrin receptor, (TrfR), which is specifically upregulated with chronic cellular iron deficiency [22–24].

2.2. Flow-Synaptometric Analysis of Striatal Nerve Terminals

Working with isolated striatal nerve terminals allows for the evaluating of the presynaptic density of adenosine receptors without the masking effect of high post-synaptic adenosine receptor levels, which is often a problem in microscopy (Figure 2A,B; see Section 4). Furthermore, this approach permits a robust and sensitive quantitative analysis of the colocalization of presynaptic markers [25]. First, we evaluated the frequency of striatal terminals (positive for synaptophysin; SYN^+) that were positive for vesicular transporter VGLUT1 ($VGLUT1^+$), VGLUT2 ($VGLUT2^+$), A_1R (A_1R^+) or $A_{2A}R$ ($A_{2A}R^+$) and the total $A_1R^+/A_{2A}R^+$ ratio. $VGLUT1^+$ and $VGLUT2^+$ striatal terminals correspond to corticostriatal and thalamo-striatal glutamatergic terminals, respectively [26–28]. The frequency of presynaptic $A_{2A}R$ labeling was about half of what we previously observed in striatal nerve terminals of CD-1 mice and Wistar rats [25], therefore most probably representing an underestimation. Unfortunately, from several other commercial antibodies, only the Nittobo/Frontiers anti-$A_{2A}R$ antibody showed sufficient selectivity in our assay when comparing its labeling to striatal nerve terminals of wild-type and $A_{2A}R$ KO mice (see Section 4). The most likely explanation for this discrepancy is that the Nittobo/Frontiers anti-$A_{2A}R$ antibody was raised against mouse $A_{2A}Rs$ and it is not equally sensitive for different rat strains (M. Watanabe, personal communication). Nevertheless, a decreased sensitivity in the detection of $A_{2A}Rs$ should not affect the conclusions related to a BID-dependent alteration of the frequency of receptors in the striatal glutamatergic terminals.

As Figure 2C demonstrates, BID did not affect the relative abundance of glutamatergic terminals in the striatum. Notably, the ratio of $VGLUT1^+$ and $VGLUT2^+$ terminals was comparable to what one can infer from electron microscopy studies [28]. There was a tendency for a decreased frequency of A_1R labelling (Figure $2D_1$) and an increased $A_{2A}R$ labelling (Figure $2D_2$) for the total synaptosomal population, but without reaching statistical significance. Nevertheless, when the ratio of A_1Rs and $A_{2A}Rs$ labeling frequencies were calculated within the same animals, there was a marked and statistically significant reduction in the $A_1R^+/A_{2A}R^+$ ratio in the BID group (Figure $2D_3$).

Table 1. Body weight and haematological parameters.

Parameter	Group	Mean	S.E.M.	p
Body Weight (g)	control BID	296.4 248.5	8.47 6.62	0.0002
Erythrocytes (10^{12}/L)	control BID	6.68 2.34	0.08 0.20	<0.0001
Hemoglobin (g/dL)	control BID	14.2 5.20	0.23 0.31	<0.0001
Hematocrit (L/L)	control BID	0.44 0.12	0.01 0.01	<0.0001
Mean Corpuscular Volume (fL)	control BID	65.1 57.3	0.54 2.76	0.0029
Mean Globular Haemoglobin (pg)	control BID	21.1 26.4	0.24 2.83	0.287
Mean Corpuscolar Haemoglobin (g/dL)	control BID	32.4 44.9	0.21 3.16	0.0093
Red Cell Distribution Width (%)	control BID	12.1 23.3	0.14 2.36	<0.0001
Leukocytes	control BID	9.28 6.43	1.06 0.97	0.0717
Segmented Neutrophils	control BID	1.21 1.09	0.16 0.27	0.8642
Eosinophils	control BID	0.08 0.054	0.05 0.03	0.4814
Lymphocytes (10^9/L)	control BID	7.51 4.99	0.81 0.66	0.0317
Monocytes (10^9/L)	control BID	0.45 0.29	0.11 0.09	0.1782
Thrombocytes (10^9/L)	control BID	777.0 1247.6	26.6 131.1	0.0215
Serum Iron Concentration (µmol/L)	control BID	44.1 4.39	2.78 0.25	<0.0001

Statistical comparisons between BID rats and controls were made with an unpaired Student's *t*-test.
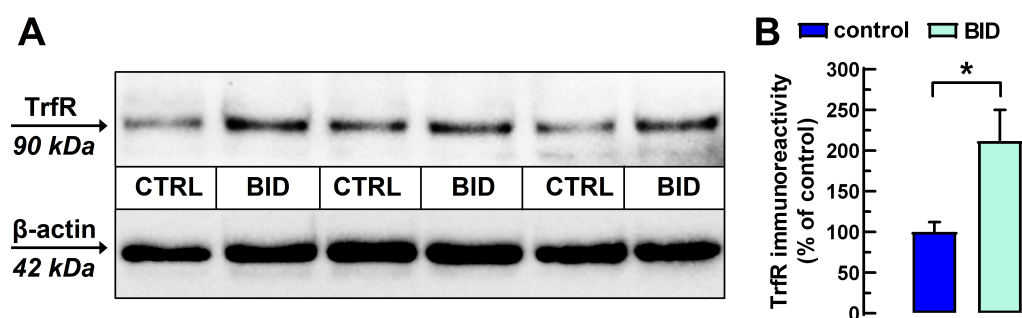

Figure 1. Increased density of transferrin receptor (TrfR) in the cerebral cortex of rats with BID as compared with controls (CTRL). (**A**) Representative blot with 10 µg proteins obtained from total cortical homogenates of three pairs of CTRL and rats with BID. (**B**) TrfR density values were compared to their respective β-actin density values after reprobing the stripped membranes and the average of TrfR/β-actin ratios from CTRL rats were taken as 100%. Statistical comparisons between rats with BID and controls were made with two-tailed unpaired Student's *t*-test (* = $p < 0.05$).
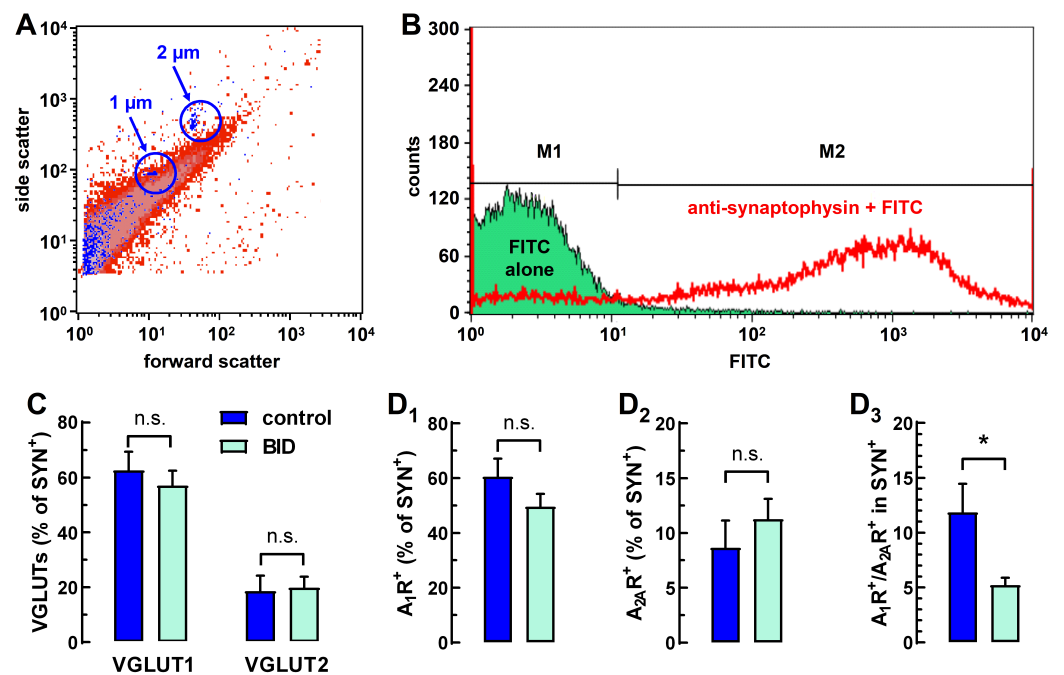
Figure 2. Localization of A_1R and $A_{2A}R$ in striatal terminals (**A**) Representative flow synaptometry dual parameter dot-plot of striatal synaptosomes for size (forward scatter; proportional to the particle size) and for complexity/granularity (side scatter). The logarithmic scales of the x and the y axes represent signal intensity in arbitrary units. Red dots represent FITC-labeled synaptosomes, while blue dots are size calibration beads. (**B**) Representative fluorescence histogram documenting the selectivity of anti-synaptophysin labeling. Specific signal (M2 region) for single-labeled synaptosomes was calculated by subtracting the percentage of labeling by the secondary antibodies alone (histogram filled with green representing synaptosomes incubated only with FITC-conjugated anti-rabbit antibody) from the percentage of labeling by the antibody of interest (histogram in red color). M1 region represents the unlabeled synaptosomes. Note that similar controls were also carried out for the other primary antibodies. (**C**) Striatal presynaptic frequency (as % of synaptophysin positive terminals, SYN^+) of vesicular glutamate transporters 1 and 2 (VGLUT1/2). (**D1**) Percentage of A_1R^+ cortico-striatal terminals, (**D2**), percentage of $A_{2A}R^+$ cortico-striatal terminals, and (**D3**) ratio between the frequency of inhibitory A_1R excitatory and the $A_{2A}R$. The inter-animal variability of A_1R and $A_{2A}R$ labelling masks the difference between control and BID in panels D_1 and D_2, while in panel D_3 there is an intra-animal normalization of $A_{2A}R$ labelling to A_1R labelling, better illustrating the effect of BID. For panels D_1–D_3, all raw data with the corresponding statistical analyses can be accessed in Supplementary Table S1. Bars represent mean + S.E.M. of n = 8–11 animals. Statistical comparisons were made with a two-tailed unpaired Student's *t*-test (n.s. = not significant; * = $p < 0.05$).

Subsequently, we calculated the labelling frequency of A_1Rs and $A_{2A}Rs$ in cortico-striatal ($VGLUT1^+$) nerve terminals. Figure 3 (panels A_1–A_3) show representative dot plots for dual-labelled synaptosomes. In synaptosomes from rats with BID, the apparent reduction in the percentage of A_1R colocalization with VGLUT1 and the increase in the percentage of $A_{2A}R$ colocalization with VGLUT1 were not statistically significant (Figure 3, panels B_1 and B_2), while the $A_1R^+/A_{2A}R^+$ ratio in $VGLUT1^+$-terminals was significantly decreased (Figure 3, panel B_3). On the other hand, BID did not significantly alter either the percentage of A_1R^+ or $A_{2A}R^+$ in thalamo-striatal ($VGLUT2^+$) nerve terminals or the $A_1R^+/A_{2A}R^+$ ratio in those terminals (Figure 4).
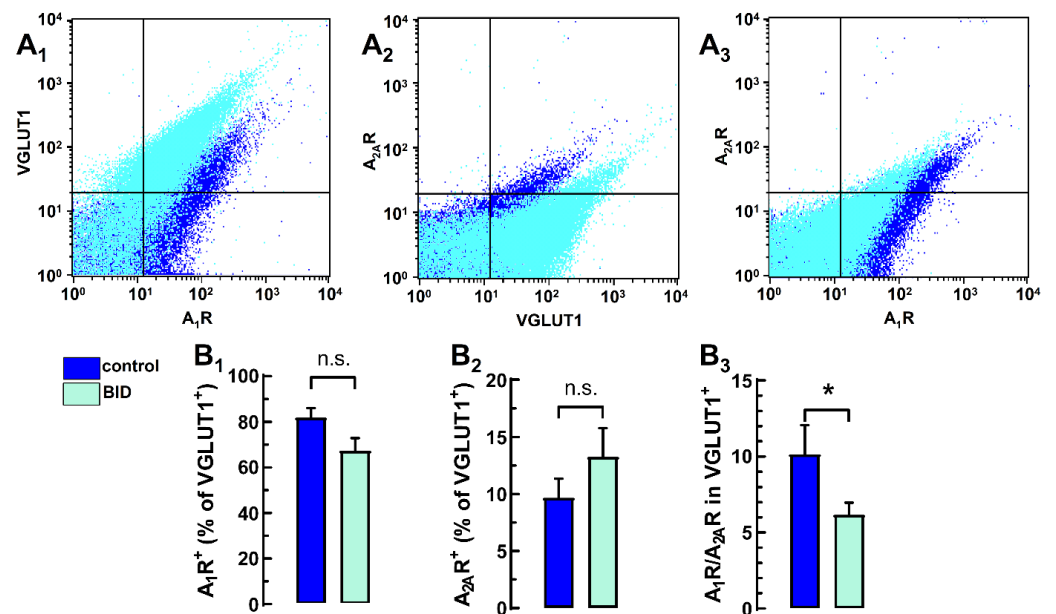
Figure 3. Localization of A_1Rs and A_{2A}Rs in cortico-striatal terminals. (A_1–A_3) Representative dot-plots showing the colocalization of VGLUT1, A_1Rs and A_{2A}Rs in the upper right quadrants in striatal synaptosomes obtained from a control rat (dark blue) and a BID animal (cyan). Logarithmic scales of the x and the y axes represent the intensity of fluorescence in arbitrary units. Percentage of cortico-striatal terminals (VGLUT1 positive) terminals that are positive for (B_1) A_1R^+, (B_2) $A_{2A}R^+$ and (B_3) ratio between the inhibitory A_1R and the excitatory $A_{2A}R$. Bars represent mean + S.E.M. of n = 8–11 animals. Statistical comparisons between rats with BID and controls were made with a two-tailed unpaired Student's *t* test (n.s. = not significant; * = $p < 0.05$).
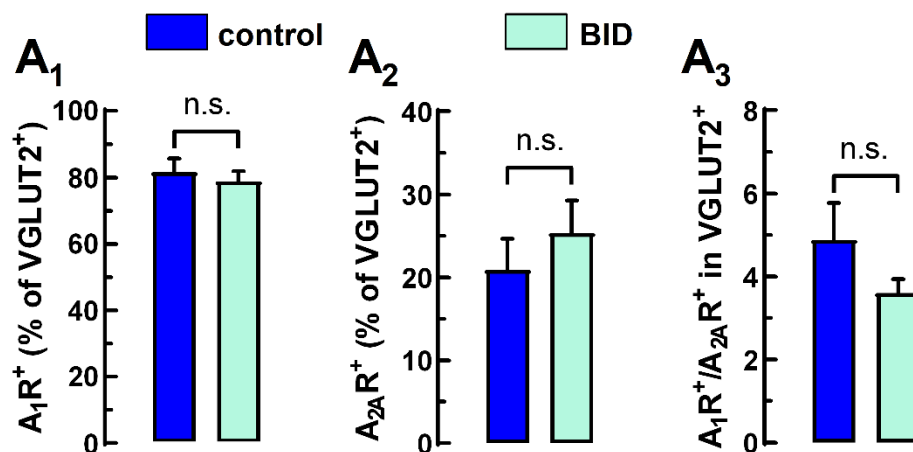

Figure 4. Localization of A_1Rs and A_{2A}Rs in thalamo-striatal terminals. Percentage of thalamo-striatal terminals (VGLUT2 positive) terminals that are positive for (A_1) A_1R^+, (A_2) $A_{2A}R^+$ and (A_3) ratio between the inhibitory A_1R and the excitatory $A_{2A}R$. Bars represent mean + S.E.M. of n = 8–11 animals. Statistical comparisons between rats with BID and controls were made with a two-tailed unpaired Student's *t*-test (n.s. = not significant).

3. Discussion

The present results provide a mechanistic explanation for the previously reported increased sensitivity of cortico-striatal glutamatergic terminals in rodents with BID [14,21]: a change in $A_1R/A_{2A}R$ stoichiometry in favor of A_{2A}Rs. Taking into account the technical limitations imposed by the relative low sensitivity of the $A_{2A}R$ antibodies, this change in $A_1R/A_{2A}R$ stoichiometry indicates that it should lead to a decrease in the population of A_{2A}Rs forming heteromers with A_1Rs in those glutamatergic terminals [17]. A_{2A}Rs have a

significant constitutive activity which is blunted upon heteromerization with A_1Rs [20]. Our theory is that A_{2A}Rs, freed from the inhibitory control of A_1Rs, recover their constitutive activity, which plays a major role in the BID-induced increased excitability of the cortico-striatal glutamatergic terminals.

We have recently found evidence for a predominant heterotetrameric structure of three different striatal A_{2A}R heteromers, constituted by A_{2A}R homodimers and either A_1R, dopamine D_2 receptor (D_2R) or cannabinoid CB_1 receptor (CB_1R) homodimers [19,20,29]. A_{2A}R-D_2R heteromers are localized postsynaptically, in striato-pallidal GABAergic neurons [11,30], while A_{2A}R-CB_1R heteromers are also localized in the cortico-striatal terminal [20,25]. It has been recently shown that, different from the A_{2A}R-A_1R heteromers, the A_{2A}R in the A_{2A}R-CB_1R heteromer preserves its constitutive activity [20]. Results of the same study suggest that the well-established cannabinoid-induced inhibition of striatal glutamate release can mostly be explained by a CB_1R-mediated counteraction of the A_{2A}R-mediated constitutive activation of adenylyl cyclase in the A_{2A}R-CB_1R heteromer [20]. A relative increase in the population of A_{2A}Rs not forming heteromers with A_1Rs would also favor a relative increase of A_{2A}Rs forming heteromers with CB_1Rs, which would also be expected to increase the population of A_{2A}Rs with constitutive activity.

Although it was initially thought that A_1R-A_{2A}R heteromers permit a fine-tune modulation by adenosine, by which low and high concentrations of adenosine preferentially activate the signaling of A_1Rs and A_{2A}Rs, respectively (see Introduction and [17]), recent results from optogenetic-microdialysis experiments with the ENT1/ENT2 inhibitor dipyridamole question this hypothesis. Thus, the direct striatal administration of dipyridamole significantly decreased basal levels of glutamate and counteracted the optogenetic-induced glutamate release by cortico-striatal terminals in both rats with BID and naïve controls [21]. According to the initial hypothesis of operation of the A_1R-A_{2A}R heteromer, the opposite effect, an increase in glutamate release, should have been expected if adenosine had reached the optimal extracellular concentration to activate the A_{2A}Rs. In fact, results also obtained with in vivo microdialysis experiments showed that exogenously added selective A_{2A}R agonists, such as CGS21680, induce glutamate release in the striatum [31,32] by directly activating presynaptic A_{2A}Rs in glutamatergic terminals [33,34]. Given dipyridamole's inability to increase glutamate release, the increase in extracellular adenosine induced by the drug seems to preferentially affect only A_1Rs and not be of sufficient concentration to activate A_{2A}Rs. An additional explanation for the preferential activation of A_1Rs vs. A_{2A}Rs with dipyridamole is the evidence for nearer co-localization of A_1R with equilibrative nucleoside transporters in specific cellular microdomains [35]. Conversely, accumulating evidence indicates that, in other microdomains, the activation of A_{2A}Rs by endogenous adenosine requires a particular pool of extracellular adenosine originated from the CD73-mediated formation of ATP-derived extracellular adenosine [36–38], in accordance with the physical association of CD73 and A_{2A}Rs in the striatum [39]. However, we would favor the first explanation for the effect of dipyridamole in cortico-striatal nerve terminals, since A_{2A}R-A_1R heteromerization implies a tight co-localization of both receptors in the same microdomain of the plasma membrane.

On the other hand, selective A_{2A}R antagonists, such as SCH-442416 or MSX-3 (prodrug of the active compound MSX-2), but not KW-6002 (istradefylline), counteract striatal glutamate release induced by electrical or optogenetic stimulation of cortico-striatal neurons [14,30,40,41]. Importantly, most A_{2A}R antagonists are inverse agonists, including SCH-442416 and MSX-2 (results in preparation), while only KW-6002 is a neutral antagonist [42], which therefore cannot counteract a constitutive activity of the A_{2A}R. Altogether, these findings with increased endogenous adenosine (with dipyridamole) and exogenous A_{2A}R ligands are compatible with the constitutive activity of A_{2A}Rs (not forming heteromers with A_1Rs) playing a more significant role in modulating (enhancing) the basal excitability of cortico-striatal terminals than its activation by endogenous adenosine. On the other hand, endogenous adenosine mostly plays a negative modulation of the excitability of cortico-striatal terminals by preferentially acting on A_1Rs (forming or not forming

heteromers with A_{2A}Rs). By promoting a preferential adenosine-mediated presynaptic activation of A_1Rs vs. A_{2A}Rs, dipyridamole could be considered as an indirect agonist of striatal presynaptic A_1Rs localized in cortico-striatal terminals.

As briefly reviewed in the Introduction, BID in rodents constitutes a model of RLS with construct validity. Rats with BID show an increased sensitivity of cortico-striatal synapses [14], which could be mechanistically related to the well-established cortical motor hyperexcitability of RLS patients [43–45]. The present study provides further support for a role of adenosine signaling in this increased sensitivity, more specifically, for a change in A_1R/A_{2A}R stoichiometry in favor of A_{2A}Rs in cortico-striatal glutamatergic terminals. In fact, previous experiments had already shown a decrease in A_1R density in the cortex and striatum and an increase in A_{2A}R density in the striatum of rodents with BID [8,9]. These neurochemical changes have not yet been reported in patients with RLS, which would further validate the rodent with BID as an animal model of RLS. The "adenosine hypothesis" of RLS, however, is supported by the efficacy of dipyridamole in treating RLS symptoms [6,7].

Co-localization of A_1Rs and A_{2A}Rs is not specific for the glutamatergic terminals of the striatum and changes in A_1R/A_{2A}R stoichiometry in favor of A_{2A}Rs in glutamatergic terminals of other brain areas can also be involved in brain conditions other than RLS. For instance, there is compelling evidence from animal models of a cortical and hippocampal upregulation of A_{2A}Rs, without a concomitant upregulation of A_1Rs, in glutamatergic synapses upon aging and Alzheimer's disease (AD) [46–49]. We propose that the relief of A_1R-mediated inhibition of the constitutive activity of the A_{2A}R in the A_1R-A_{2A}R heteromer represents a common mechanism involved in neuropsychiatric conditions with increased glutamatergic transmission. Therefore, blocking the constitutive activity of presynaptic A_{2A}Rs with selective inverse agonists or increasing the activation of presynaptic A_1Rs with a preferential indirect A_1R agonists like dipyridamole could provide valuable therapeutic approaches for those neuropsychiatric disorders.

4. Materials and Methods

4.1. Animals

All experiments were performed in accordance with the local animal welfare committee (Centre for Neuroscience and Cell Biology, University of Coimbra, Portugal), European Union guidelines and the Federation of Laboratory Animal Science Associations (FELASA) and were approved by the Animal Care Committee (ORBEA) of the Center for Neuroscience and Cell Biology of the University of Coimbra, Coimbra, Portugal (license number 257). Sprague-Dawley rats were purchased from Charles-River (Écully, France) for breeding. Animals throughout the study were housed with 12 h light on/off cycles under controlled temperature (23 ± 2 °C) and *ad libitum* access to food and water. All efforts were made to minimize the number of animals used and to minimize their stress and discomfort. On post-natal day 16 (PND16), the food of the lactating dams was changed from regular rat chow to a rat chow containing 48 ppm or mg/kg Fe^{2+} (code: TD.80396; ssniff Spezialdiäten GmbH, Soest, Germany). On PND21, the litter was weaned, and 19 male pups were randomly assigned to the adjusted control group (receiving chow with 48 ppm Fe^{2+}) and BID group (receiving the modified TD.80396 diet containing residual, 6–8 ppm Fe^{3+}). Two to three pups were housed per cage.

4.2. Determination of Peripheral Iron Deficiency and Bid

28 days after the initiation of the iron diet, rats were weighed, then deeply anesthetized with halothane in a chamber (no reaction to tail pinch or handling, while still breathing), and decapitated with a stainless-steel guillotine for immediate tissue collection in ice-cold sucrose solution. Some of the dissected brain parts were snap-frozen in liquid nitrogen, while the striata were used instantly for the preparation of purified synaptosomes (see below), which were then snap-frozen and stored at −80 °C until use within a month. In addition, the blood was collected in tubes with 0.5 M K_2EDTA to perform supplementary

hematological analysis by a local external laboratory (Laboratory of Beatriz Godinho, Coimbra, Portugal).

4.3. Purified Synaptosomes

4.3.1. Preparation of S1 Fraction

Synaptosome preparation and purification was carried out according to the protocol described by Dunkley et al. [50], with some changes introduced by us [25]. The brains were quickly collected in an ice-cold solution of 320 mM sucrose, 1 mM EDTA and 5 mM Tris, pH 7.4. The pair of striata were isolated and homogenized, using a Potter Teflon, in 6 mL sucrose. This homogenate was divided into three 2 mL Eppendorf tubes, and centrifuged at 4000 g for 5 min. The first supernatants (S1) of the first two low-speed centrifugations were layered on top of the discontinuous Percoll gradient for purification.

4.3.2. Discontinuous Percoll Gradient

Percoll gradients (Percoll diluted in the above sucrose solution to 3%, 10%, 15% and 23%) were prepared as detailed before [25,50]. In 15 mL centrifuge tubes, 2 mL of the S1 synaptosomal fraction were layered gently with a peristaltic pump on top of the Percoll gradients. The gradients were centrifuged at 25,000 g for 11 min at 4 °C. The purified synaptosomes were removed between the 15% and 23% layers and subsequently, diluted to 15 mL with HEPES buffered medium (HBM) with the following constitution: 140 mM NaCl, 5 mM KCl, 5 mM $NaHCO_3$, 1.2 mM NaH_2PO_4, 1.2 mM $MgCl_2$, 10 mM glucose, and 10 mM HEPES, pH 7.4. The samples were centrifuged at 22,000 g for 11 min at 4 °C, the pellet was collected, diluted in 2 mL of HBM and centrifuged at 5000 g for 11 min at 4 °C and the final pellet was snap-frozen in liquid nitrogen and stored at −80 °C until use.

4.3.3. Immunolabeling and Flow Synaptometry Analysis

Immunochemical labeling was performed according to a method for staining of intracellular antigens [25,51] for flow cytometry. The pellets obtained after purification in gradients were fixed in 1 mL of 0.25% paraformaldehyde in phosphate buffered saline (PBS; 135 mM NaCl, 1.3 mM KCl, 3.2 mM NaH_2PO_4, 0.5 mM KH_2PO_4 and 10 mM EDTA) for 1 h at 4 °C. After fixation, they were centrifuged at 5000 g for 3 min at 4 °C. The pellet was incubated with PBS with 0.2% Tween 20 for 15 min at 37 °C and then centrifuged at 5000 g, and subsequently, washed and pelleted with 0.5 mL of PBS for 3 min at 4 °C. The resulting pellet was resuspended and diluted in ~200 μL PBS. For immunolabeling, 5 μL of these resuspended synaptosomes were incubated with 100 μL of primary and secondary antibodies, all diluted in PBS with 2% normal goat serum (Jackson Immunoresearch, West Grove, PA, USA), for 30 min at 4 °C. As primary antibodies, we used rabbit monoclonal anti-synaptophysin (1:300; Synaptic Systems, Goettingen, Germany), mouse monoclonal anti-VGLUT1 (1:100; Synaptic Systems), mouse monoclonal anti-VGLUT2 (1:10,000; Synaptic Systems), rabbit polyclonal anti-A_1R (1:300; Invitrogen, Walthan, MA, USA) and guinea pig polyclonal anti-A_{2A}R (1:30; Frontiers/Nittobo, Tokyo, Japan). As secondary antibodies, we used goat IgG anti-mouse Cy3 (1:200; Jackson Immunoresearch), goat IgG anti-rabbit FITC (1:200; Jackson Immunoresearch) and goat IgG anti-guinea pig Cy5 (1:200; Abcam, Cambridge, UK). The optimal dilution for the primary and secondary antibodies was determined previously (Ferreira et al., 2015). After each incubation, three washes were carried out for 3 min each, with PBS 0.2% Tween 20, at 5000 g at 4 °C. Negative controls without primary antibodies were also carried out, containing only synaptosomes and secondary antibodies.

4.3.4. Detection of Synaptosomes and Data Analysis

Labeled synaptosomal pellets were then resuspended in PBS and were analyzed in a FACSCalibur flow cytometer (four channels; Becton, Dickinson and Company, East Rutherford, NJ, USA). The right dilution for each sample was adjusted to work within a count of 300–400 events per second. Approximately 30,000 events were collected for

analysis. From earlier electron microscopy studies (see for instance ref. [28]), we inferred that the size of striatal glutamatergic synapses falls predominantly between 0.5 and 2 μm. Thus, with the help of the Invitrogen Flow Cytometry Sub-micron Particle Size Reference Kit, we calibrated the gating of our equipment for this size range (Figure 2A). Data analysis was performed using BD Cell Quest Pro software. Data were plotted in a dual-parameter dot plot to analyze the percent of co-localization through the upper right quadrant. A threshold was set on forward light scatter to exclude debris. To correct for spectral overlap during multicolor flow cytometry experiments, color compensation was performed. The specific labeling of each sample is calculated by subtracting the percentage of labeling the sample with that of the respective controls and with the percentage of PBS debris (Figure 2B).

4.4. Western Blotting

To test the effectiveness of the BID protocol on the brain, cortical samples of both the control and the BID group were homogenized and sonicated in 1% SDS, then proteins were quantified with the colorimetric bicinchoninic acid (BCA) assay. Next, the samples were denatured with SDS sample buffer (500 mM Tris, 600 mM dithiothreitol, 10.3% SDS, 30% glycerol and 0.012% bromophenol) at 70 °C for 20 min. From each sample, 10 μg of protein was loaded into the gels and subsequently separated by polyacrylamide gel electrophoresis (SDS-PAGE), using a 4% stacking gel (4% bis-acrylamide, tris-HCl (0.5 M, pH 6.8), 10% SDS, 10% ammonium persulfate, 1% tetramethylethylenediamine (TEMED) and a 10% resolving gel 10% bis-acrylamide, tris-HCl (1.5 M, pH 8.8), 10% SDS, 10% ammonium persulfate, 1% TEMED), first at 60 V for 15 min and then at 120 V for 60 min. Then, proteins were transferred to nitrocellulose membranes at 0.75 A for 2 h, at 4 °C with agitation, with CAPS solution (*N*-cyclohexyl-3-aminopropanesulfonic acid) buffered solution with methanol (10 mM CAPS; 10% methanol, pH 11.0). The membranes were blocked with 3% bovine albumin serum (BSA; Merck Biosciences, Darmstadt, Germany) in Tris-buffered saline (10 mM Tris; 150 mM NaCl) containing 0.1% Tween-20 (TBS-T) for 1 h at room temperature. The membranes were then incubated with a monoclonal mouse anti-transferrin receptor antibody (1:2000; Invitrogen), overnight at 4 °C. After incubation, membranes were washed for 3 × 5 min in TBS-T and then incubated with secondary antibody (goat anti-rabbit IgG peroxidase conjugated; Thermo Scientific, Walthan, MA, USA) with 3% BSA for 2 h at room temperature. After washing three times for 5 min, the membranes were processed for protein detection using an enhanced chemiluminescence kit (Pierce™ECL Western Blotting Substrate, Thermo Scientific 32106), and the bands visualized on a on a ChemiDoc Plus imaging system (BioRad, Hercules, CA, USA). After stripping, the membranes were reprobed with an anti-β-actin antibody (1:20,000; Merck Biosciences) for normalization of protein density. Quantification of the optical density of the bands was performed using the Image Lab™ software version 6.0.1 (BioRad).

Supplementary Materials: The following supporting information can be downloaded at Table S1: Data and statistics for Figure 2.

Author Contributions: Conceptualization, S.G.F., C.Q., F.C., A.K. and S.F.; methodology, M.S.R. and S.G.F.; analysis, M.S.R. and S.G.F. and A.K.; resources, A.K. and S.F.; writing—original draft preparation, S.G.F., A.K. and S.F.; writing—review and editing, S.G.F., C.Q., C.J.E., D.G.-B., R.A.C., F.C., A.K. and S.F.; supervision, S.G.F., C.Q., A.K. and S.F.; funding acquisition, A.K. and S.F. All authors have read and agreed to the published version of the manuscript.

Institutional Review Board Statement: All experiments were performed in accordance with the local animal welfare committee (Centre for Neuroscience and Cell Biology, University of Coimbra, Portu-gal), European Union guidelines and the Federation of Laboratory Ani-mal Science Associations (FELASA) and were approved by the Animal Care Commit-tee (ORBEA) of the Center for Neuroscience and Cell Biology of the University of Coimbra, Coimbra, Portugal (license number 257).

Informed Consent Statement: Not applicable.

Data Availability Statement: Not applicable.

Conflicts of Interest: The authors declare that they have no conflict of interest.

Sample Availability: Not applicable.

References

1. Allen, R.P.; Picchietti, D.L.; Garcia-Borreguero, D.; Ondo, W.G.; Walters, A.S.; Winkelman, J.W.; Zucconi, M.; Ferri, R.; Trenkwalder, C.; Lee, H.B. Restless Legs Syndrome Study Group. Restless legs syndrome/Willis–Ekbom disease diagnostic criteria: Updated International Restless Legs Syndrome Study Group (IRLSSG) consensus criteria—History, rationale, description, and significance. *Sleep Med.* **2014**, *15*, 860–873. [CrossRef] [PubMed]
2. Manconi, M.; Garcia-Borreguero, D.; Schormair, B.; Videnovic, A.; Berger, K.; Ferri, R.; Dauvilliers, Y. Restless legs syndrome. *Nat. Rev. Dis. Primers* **2021**, *7*, 80. [CrossRef] [PubMed]
3. Ferré, S.; García-Borreguero, D.; Allen, R.P.; Earley, C.J. New Insights into the Neurobiology of Restless Legs Syndrome. *Neuroscientist* **2018**, *25*, 113–125. [CrossRef] [PubMed]
4. Earley, C.J.; Connor, J.; Garcia-Borreguero, D.; Jenner, P.; Winkelman, J.; Zee, P.C.; Allen, R. Altered Brain iron homeostasis and dopaminergic function in Restless Legs Syndrome (Willis–Ekbom Disease). *Sleep Med.* **2014**, *15*, 1288–1301. [CrossRef]
5. Ferré, S.; Quiroz, C.; Guitart, X.; Rea, W.; Seyedian, A.; Moreno, E.; Casadó-Anguera, V.; Díaz-Ríos, M.; Casadó, V.; Clemens, S.; et al. Pivotal Role of Adenosine Neurotransmission in Restless Legs Syndrome. *Front. Neurosci.* **2018**, *11*, 722. [CrossRef]
6. Garcia-Borreguero, D.; Guitart, X.; Garcia Malo, C.; Cano-Pumarega, I.; Granizo, J.J.; Ferré, S. Treatment of restless legs syndrome/Willis-Ekbom disease with the non-selective ENT1/ENT2 inhibitor dipyridamole: Testing the adenosine hypothesis. *Sleep Med.* **2018**, *45*, 94–97. [CrossRef]
7. Garcia-Borreguero, D.; Garcia-Malo, C.; Granizo, J.J.; Ferré, S. A Randomized, Placebo-Controlled Crossover Study with Dipyridamole for Restless Legs Syndrome. *Mov. Disord.* **2021**, *36*, 2387–2392. [CrossRef]
8. Quiroz, C.; Pearson, V.; Gulyani, S.; Allen, R.; Earley, C.; Ferré, S. Up-regulation of striatal adenosine A2A receptors with iron deficiency in rats: Effects on locomotion and cortico-striatal neurotransmission. *Exp. Neurol.* **2010**, *224*, 292–298. [CrossRef]
9. Quiroz, C.; Gulyani, S.; Ruiqian, W.; Bonaventura, J.; Cutler, R.; Pearson, V.; Allen, R.P.; Earley, C.J.; Mattson, M.P.; Ferré, S. Adenosine receptors as markers of brain iron deficiency: Implications for Restless Legs Syndrome. *Neuropharmacology* **2016**, *111*, 160–168. [CrossRef]
10. Dunwiddie, T.V.; Masino, S.A. The Role and Regulation of Adenosine in the Central Nervous System. *Annu. Rev. Neurosci.* **2001**, *24*, 31–55. [CrossRef]
11. Ferré, S.; Fuxe, K.; Fredholm, B.B.; Morelli, M.; Popoli, P. Adenosine-dopamine receptor-receptor interactions as an integra-tive mechanism in the basal ganglia. *Trends Neurosci.* **1997**, *20*, 482–487. [CrossRef]
12. Borycz, J.; Pereira, M.F.; Melani, A.; Rodrigues, R.J.; Köfalvi, A.; Panlilio, L.; Pedata, F.; Goldberg, S.R.; Cunha, R.A.; Ferré, S. Differential glutamate-dependent and glutamate-independent adenosine A1 receptor-mediated modulation of dopamine re-lease in different striatal compartments. *J. Neurochem.* **2007**, *101*, 355–363. [CrossRef]
13. Brown, R.; Basheer, R.; McKenna, J.; Strecker, R.E.; McCarley, R. Control of Sleep and Wakefulness. *Physiol. Rev.* **2012**, *92*, 1087–1187. [CrossRef] [PubMed]
14. Yepes, G.; Guitart, X.; Rea, W.; Newman, A.H.; Allen, R.P.; Earley, C.J.; Quiroz, C.; Ferré, S. Targeting hypersensitive cor-ticostriatal terminals in restless legs syndrome. *Ann. Neurol.* **2017**, *82*, 951–960. [CrossRef] [PubMed]
15. Silber, M.H.; Buchfuhrer, M.J.; Earley, C.J.; Koo, B.B.; Manconi, M.; Winkelman, J.W. The management of Restless Legs Syndrome: An updated algorithm. *Mayo Clin. Proc.* **2021**, *96*, 1921–1937. [CrossRef] [PubMed]
16. Bonaventura, J.; Quiroz, C.; Cai, N.S.; Rubinstein, M.; Tanda, G.; Ferré, S. Key role of the dopamine D4 receptor in the mod-ulation of corticostriatal glutamatergic neurotransmission. *Sci. Adv.* **2017**, *3*, e1601631. [CrossRef]
17. Ciruela, F.; Casadó, V.; Rodrigues, R.; Luján, R.; Burgueño, J.; Canals, M.; Borycz, J.; Rebola, N.; Goldberg, S.R.; Mallol, J.; et al. Presynaptic Control of Striatal Glutamatergic Neurotransmission by Adenosine A1-A2A Receptor Heteromers. *J. Neurosci.* **2006**, *26*, 2080–2087. [CrossRef]
18. Lopes, L.; Cunha, R.; Kull, B.; Fredholm, B.; Ribeiro, J. Adenosine A2A receptor facilitation of hippocampal synaptic transmission is dependent on tonic A1 receptor inhibition. *Neuroscience* **2002**, *112*, 319–329. [CrossRef]
19. Navarro, G.; Cordomí, A.; Brugarolas, M.; Moreno, E.; Aguinaga, D.; Pérez-Benito, L.; Ferre, S.; Cortés, A.; Casadó, V.; Mallol, J.; et al. Cross-communication between Gi and Gs in a G-protein-coupled receptor heterotetramer guided by a receptor C-terminal domain. *BMC Biol.* **2018**, *16*, 1–15. [CrossRef]

20. Köfalvi, A.; Moreno, E.; Cordomí, A.; Cai, N.S.; Fernández-Dueñas, V.; Ferreira, S.G.; Guixà-González, R.; Sánchez-Soto, M.; Yano, H.; Casadó-Anguera, V.; et al. Control of glutamate release by complexes of adenosine and cannabinoid receptors. *BMC Biol.* **2020**, *18*, 9. [CrossRef]

21. Ferré, S.; Quiroz, C.; Rea, W.; Guitart, X.; García-Borreguero, D. Adenosine mechanisms and hypersensitive corticostriatal terminals in restless legs syndrome. Rationale for the use of inhibitors of adenosine transport. *Adv. Pharmacol.* **2019**, *84*, 3–19. [CrossRef] [PubMed]

22. Lok, C.; Loh, T. Regulation of transferrin function and expression: Review and update. *Biol. Signals Recept.* **1998**, *7*, 157–178. [CrossRef] [PubMed]

23. Han, J.; Day, J.R.; Connor, J.R.; Beard, J.L. Gene expression of transferrin and transferrin receptor in brains of control vs. iron-deficient rats. *Nutr. Neurosci.* **2003**, *6*, 1–10.

24. Gulyani, S.; Earley, C.J.; Camandola, S.; Maudsley, S.; Ferré, S.; Mughal, M.R.; Martin, B.; Cheng, A.; Gleichmann, M.; Jones, B.C.; et al. Diminished iron concentrations increase adenosine A2A receptor levels in mouse striatum and cultured human neuroblastoma cells. *Exp. Neurol.* **2009**, *215*, 236–242. [CrossRef]

25. Ferreira, S.G.; Gonçalves, F.Q.; Marques, J.M.; Tomé, R.; Rodrigues, R.J.; Nunes-Correia, I.; Ledent, C.; Harkany, T.; Venance, L.; A Cunha, R.; et al. Presynaptic adenosine A_{2A} receptors dampen cannabinoid CB_1 receptor-mediated inhibition of corticostriatal glutamatergic transmission. *J. Cereb. Blood Flow Metab.* **2015**, *172*, 1074–1086. [CrossRef]

26. Fujiyama, F.; Kuramoto, E.; Okamoto, K.; Hioki, H.; Furuta, T.; Zhou, L.; Nomura, S.; Kaneko, T. Presynaptic localization of an AMPA-type glutamate receptor in corticostriatal and thalamostriatal axon terminals. *Eur. J. Neurosci.* **2004**, *20*, 3322–3330. [CrossRef] [PubMed]

27. Fujiyama, F.; Unzai, T.; Nakamura, K.; Nomura, S.; Kaneko, T. Difference in organization of corticostriatal and thalamostri-atal synapses between patch and matrix compartments of rat neostriatum. *Eur. J. Neurosci.* **2006**, *24*, 2813–2824. [CrossRef] [PubMed]

28. Raju, D.V.; Smith, Y. Differential Localization of Vesicular Glutamate Transporters 1 and 2 in the Rat Striatum. *Neuroscience* **2006**, 601–610. [CrossRef]

29. Navarro, G.; Cordomí, A.; Casadó-Anguera, V.; Moreno, E.; Cai, N.-S.; Cortés, A.; Canela, E.I.; Dessauer, C.W.; Casadó, V.; Pardo, L.; et al. Evidence for functional pre-coupled complexes of receptor heteromers and adenylyl cyclase. *Nat. Commun.* **2018**, *9*, 1–12. [CrossRef]

30. Ferré, S.; Bonaventura, J.; Zhu, W.; Hatcher-Solis, C.; Taura, J.; Quiroz, C.; Cai, N.-S.; Moreno, E.; Casadó-Anguera, V.; Kravitz, A.V.; et al. Essential Control of the Function of the Striatopallidal Neuron by Pre-coupled Complexes of Adenosine A_{2A}-Dopamine D_2 Receptor Heterotetramers and Adenylyl Cyclase. *Front. Pharmacol.* **2018**, *9*, 243. [CrossRef]

31. Popoli, P.; Betto, P.; Reggio, R.; Ricciarello, G. Adenosine A_{2A} receptor stimulation enhances striatal extracellular glutamate levels in rats. *Eur. J. Pharmacol.* **1995**, *287*, 215–217. [CrossRef]

32. Quarta, D.; Borycz, J.; Solinas, M.; Patkar, K.; Hockemeyer, J.; Ciruela, F.; Lluis, C.; Franco, R.; Woods, A.S.; Goldberg, S.R.; et al. Adenosine receptor-mediated modulation of dopamine release in the nucleus accumbens depends on glutamate neurotransmission and N-methyl-d-aspartate receptor stimulation. *J. Neurochem.* **2004**, *91*, 873–880. [CrossRef] [PubMed]

33. Rodrigues, R.J.; Alfaro, T.M.; Rebola, N.; Oliveira, C.R.; Cunha, R.A. Co-localization and functional interaction between adenosine A_{2A} and metabotropic group 5 receptors in glutamatergic nerve terminals of the rat striatum. *J. Neurochem.* **2004**, *92*, 433–441. [CrossRef]

34. Shen, H.Y.; Canas, P.M.; Garcia-Sanz, P.; Lan, J.Q.; Boison, D.; Moratalla, R.; Cunha, R.A.; Chen, J.F. Adenosine A_{2A} receptors in striatal glutamatergic terminals and GABAergic neurons oppositely modulate psychostimulant action and DARPP-32 phosphorylation. *PLoS ONE* **2013**, *8*, e80902. [CrossRef] [PubMed]

35. Cunha, R.A. How does adenosine control neuronal dysfunction and neurodegeneration? *J. Neurochem.* **2016**, *139*, 1019–1055. [CrossRef]

36. Carmo, M.; Gonçalves, F.Q.; Canas, P.M.; Oses, J.P.; Fernandes, F.D.; Duarte, F.V.; Palmeira, C.M.; Tomé, A.R.; Agostinho, P.; Andrade, G.M.; et al. Enhanced ATP release and CD73-mediated adenosine formation sustain adenosine A_{2A} receptor over-activation in a rat model of Parkinson's disease. *Br. J. Pharmacol.* **2019**, *176*, 3666–3680. [CrossRef] [PubMed]

37. Gonçalves, F.Q.; Lopes, J.P.; Silva, H.B.; Lemos, C.; Silva, A.C.; Gonçalves, N.; Tomé, Â.R.; Ferreira, S.G.; Canas, P.M.; Rial, D.; et al. Synaptic and memory dysfunction in a β-amyloid model of early Alzheimer's disease depends on increased formation of ATP-derived extracellular adenosine. *Neurobiol. Dis.* **2019**, *132*, 104570. [CrossRef]

38. Augusto, E.; Gonçalves, F.Q.; Real, J.E.; Silva, H.B.; Pochmann, D.; Silva, T.S.; Matos, M.; Gonçalves, N.; Tomé, Â.R.; Chen, J.F.; et al. Increased ATP release and CD73-mediated adenosine A2A receptor activation mediate convulsion-associated neuronal damage and hippocampal dysfunction. *Neurobiol. Dis.* **2021**, *157*, 105441. [CrossRef]

39. Augusto, E.; Matos, M.; Sévigny, J.; El-Tayeb, A.; Bynoe, M.S.; Müller, C.E.; Cunha, R.A.; Chen, J.-F. Ecto-5′-nucleotidase (CD73)-mediated formation of adenosine is critical for the striatal adenosine A_{2A} receptor functions. *J. Neurosci.* **2013**, *33*, 11390–11399. [CrossRef]

40. Orrù, M.; Bakešová, J.; Brugarolas, M.; Quiroz, C.; Beaumont, V.; Goldberg, S.R.; Lluis, C.; Cortés, A.; Franco, R.; Casadó, V.; et al. Striatal Pre- and Postsynaptic Profile of Adenosine A_{2A} Receptor Antagonists. *PLoS ONE* **2011**, *6*, e16088. [CrossRef]

41. Quiroz, C.; Orrù, M.; Rea, W.; Ciudad-Roberts, A.; Yepes, G.; Britt, J.P.; Ferré, S. Local Control of Extracellular Dopamine Levels in the Medial Nucleus Accumbens by a Glutamatergic Projection from the Infralimbic Cortex. *J. Neurosci.* **2016**, *36*, 851–859. [CrossRef] [PubMed]

42. Bennett, K.A.; Tehan, B.; Lebon, G.; Tate, C.G.; Weir, M.; Marshall, F.H.; Langmead, C. Pharmacology and Structure of Isolated Conformations of the Adenosine A$_{2A}$ Receptor Define Ligand Efficacy. *Mol. Pharmacol.* **2013**, *83*, 949–958. [CrossRef] [PubMed]

43. Tergau, F.; Wischer, S.; Paulus, W. Motor system excitability in patients with restless legs syndrome. *Neurology* **1999**, *52*, 1060. [CrossRef] [PubMed]

44. Scalise, A.; Cadore, I.P.; Gigli, G.L. Motor cortex excitability in restless legs syndrome. *Sleep Med.* **2004**, *5*, 393–396. [CrossRef] [PubMed]

45. Lanza, G.; Cantone, M.; Lanuzza, B.; Pennisi, M.; Bella, R.; Pennisi, G.; Ferri, R. Distinctive patterns of cortical excitability to transcranial magnetic stimulation in obstructive sleep apnea syndrome, restless legs syndrome, insomnia, and sleep deprivation. *Sleep Med. Rev.* **2015**, *19*, 39–50. [CrossRef]

46. Lopes, L.V.; Cunha, R.; Ribeiro, J. Increase in the Number, G Protein Coupling, and Efficiency of Facilitatory Adenosine A$_{2A}$ Receptors in the Limbic Cortex, but not Striatum, of Aged Rats. *J. Neurochem.* **2002**, *73*, 1733–1738. [CrossRef]

47. Sebastião, A.M.; Cunha, R.A.; de Mendonça, A.; Ribeiro, J.A. Modification of adenosine modulation of synaptic transmission in the hippocampus of aged rats. *Br. J. Pharmacol.* **2000**, *131*, 1629–1634. [CrossRef] [PubMed]

48. Rebola, N.; Sebastião, A.M.; de Mendonca, A.; Oliveira, C.R.; Ribeiro, J.A.; Cunha, R.A. Enhanced adenosine A$_{2A}$ receptor facilitation of synaptic transmission in the hippocampus of aged rats. *J. Neurophysiol.* **2003**, *90*, 1295–1303. [CrossRef]

49. Temido-Ferreira, M.; Ferreira, D.G.; Batalha, V.L.; Marques-Morgado, I.; Coelho, J.E.; Pereira, P.; Gomes, R.; Pinto, A.; Car-valho, S.; Canas, P.M.; et al. Age-related shift in LTD is dependent on neuronal adenosine A$_{2A}$ receptors interplay with mGluR5 and NMDA receptors. *Mol. Psychiatry* **2020**, *25*, 1876–1900. [CrossRef]

50. Dunkley, P.R.; E Jarvie, P.; Robinson, P.J. A rapid Percoll gradient procedure for preparation of synaptosomes. *Nat. Protoc.* **2008**, *3*, 1718–1728. [CrossRef]

51. Gylys, K.H.; Fein, J.A.; Cole, G.M. Quantitative characterization of crude synaptosomal fraction (P-2) components by flow cytometry. *J. Neurosci. Res.* **2000**, *61*, 186–192. [CrossRef]